ChemComm

RSC Publishing

COMMUNICATION

View Article Online
View Journal | View Issue

Cite this: *Chem. Commun.*, 2013, **49**, 11698

Received 4th September 2013,
Accepted 22nd October 2013

DOI: 10.1039/c3cc46744a

www.rsc.org/chemcomm

Pyrene-imidazolium complexed graphene for the selective fluorescent detection of G-quadruplex forming DNA†

Seung Jin Moon,[a] So Hyeon Park,[a] Justyn Jaworski*[bc] and Jong Hwa Jung*[a]

A unique system has been developed for quantifying G-quadruplex forming DNA down to picomolar levels for future applications in telomeric assessment. Pyrene-imidazolium captured in high amounts on the surface of reduced graphene oxide shells allows specific DNA sequence detection by complex formation resulting in release and fluorescence enhancement of pyrene-imidazolium.

It is widely accepted that the DNA–protein complexes, known as telomeres, have a key influence on the state and lifetime of normal cells as well as cancers. Located at the end of the chromosome as a capping sequence, the length and interactions between telomeric DNA may ultimately dictate cell growth and death.[1] The guanine rich sequences of human telomeric DNA, for example $(TTAGGG)_n$, are of particular interest as these terminal sequences are capable of forming G-quadruplex structures that may inhibit telomerase extension of the repeating telomeric DNA, thereby allowing cell death to occur.[2] Stabilization of the G-quadruplex structure may prevent the unwanted characteristic immortality of cancer cells; hence, G-quadruplex stabilizers are actively under research as anti-tumor therapeutics.[3–5]

While G-quadruplex DNA structures have been extensively utilized as sensors due to their affinity for metal ions,[6] very little literature exists on the detection of G-quadruplex forming DNA itself.[7,8] Estimation of telomeric DNA length typically requires laborious digest methods to determine the mean terminal restriction fragment length,[9] or alternatively fluorescence *in situ* hybridization has been used to obtain the relative number of DNA repeats but only for a predetermined sequence.[10] Therefore, a need still exists for the development of a detection system with selectivity for the presence of quadruplex forming DNA, or more importantly the length of the telomeric DNA. Such a system could provide critical information on the replicative history of the cells, thereby offering an indication of their fate.[11]

In the following work, we reveal a sensitive and selective strategy for identifying DNA capable of forming a G-quadruplex. By specifically making use of graphene encapsulation of silica nanoparticle molds to provide a hollow graphene shell, we produced a high surface area platform for capture and fluorescence quenching of pyrene-appended imidazolium (referred to as SiO_2@rGO-**PI**). Importantly, liberation of pyrene-appended imidazolium (**PI**) from the graphene shell (SiO_2@rGO) can occur in the presence of even trace concentrations of G-quadruplex forming DNA. As a result, the **PI** bound complex with DNA emits a high fluorescence signal in the solution, which we confirmed by spectral observation to be proportional to the concentration of G-quadruplex forming DNA. **PI** has previously shown several important properties thereby inspiring its use for our detection scheme. For instance, **PI** will selectively destabilize G-quadruplex forming dsDNA sequences resulting in complex formation with one of the ssDNA strands to create a G-quartet structure (hydrogen bonding among four guanine bases), where the formation of this unique structure induces fluorescence emission from the excited state complex.[12] In our system, this complex formation allows the **PI** to be released from the graphene shell allowing fluorescence-enhanced detection that is both sensitive and selective to G-quadruplex forming DNA. The confirmation resulting from G-quartet formation, as induced by **PI**, results in excimer enhancement of the pyrene moiety of **PI** as observed by the fluorescence peak at 550 nm.

Prior studies making use of graphene encapsulation of nanoparticles have provided functional, high surface area structures with applicability in enantioselective separation systems,[13] hybrid biomaterials for bone growth,[14] multifunctional probes[15] and sensor development.[16] The significant enhancement in the surface area-to-volume ratio seen in graphene encapsulated silica nanoparticles has proven particularly useful for FET-type protein sensors resulting in significantly improved detection limits.[17] From a DNA sensor perspective, graphene has previously demonstrated the capability to bind with ssDNA *via* non-covalent interactions with aromatic nucleobases;[18] however, quadruplex

[a] *Department of Chemistry and Research Institute of Natural Sciences, Gyeongsang National University, Jinju, South Korea. E-mail: jonghwa@gnu.ac.kr; Fax: +82-055-758-6027; Tel: +82-055-772-1488*

[b] *Department of Chemical Engineering, Hanyang University, Seoul, South Korea. E-mail: justynj@hanyang.ac.kr; Fax: +82-02-2220-1935; Tel: +82-02-2220-2339*

[c] *Institute of Nano Science and Technology, 222 Wangsimni-ro, Seoul, South Korea*

† Electronic supplementary information (ESI) available: Detailed experimental and synthesis procedures as well as sequence details and XPS. See DOI: 10.1039/c3cc46744a

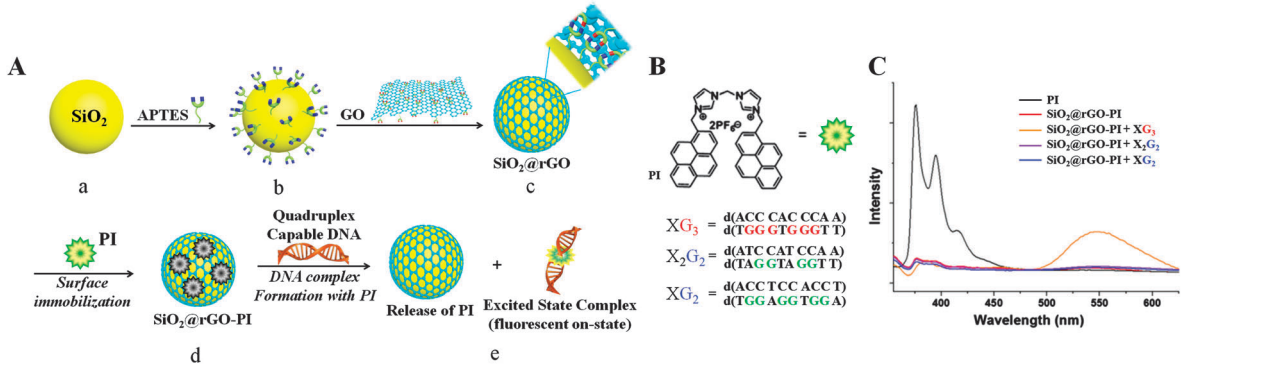

Fig. 1 (A) Schematic of the preparation method for SiO_2@rGO-**PI**; (a) SiO_2 particles, (b) amino group functionalized SiO_2 particles, (c) rGO wrapped SiO_2 particles, (d) **PI** adsorbed onto SiO_2@rGO and (e) **PI** released from SiO_2@rGO. (B) Chemical structure of **PI** and the various DNA used in this study. (C) Fluorescence spectra of **PI**, SiO_2@rGO-**PI**, and also SiO_2@rGO-**PI** in the presence of various DNA.

DNA, in contrast, was shown to exhibit dramatically decreased binding.[19]

In our system, π–π stacking interactions between the aromatic surfaces of graphene and pyrene allow the capture of **PI** on the surface of the hollow graphene shell (Fig. 1). This close proximity to graphene results in a fluorescently quenched state for the **PI** moiety. This ability of graphene to be a good energy acceptor has encouraged its use in a number of sensing platforms where high fluorescence quenching efficiency is required.[18] Disassociation of **PI** motifs from the surface was found to occur selectively after exposure to dsDNA possessing the characteristic G-quadruplex forming sequence (XG_3). As a result, significant fluorescent enhancement was observed with the release of the **PI**–DNA complex. In brief, our results demonstrate a selective detection limit of quadruplex forming dsDNA as low as 20 pM for a 10-mer of dsDNA. Interestingly, an increase in the fluorescence signal was found when using longer stretches of this repeat sequence. In addition, non-specific sequences (*i.e.*, XG_2 and X_2G_2) hardly affected the quenching of **PI** by graphene, since a selective G-quartet complex formation would be required to release the moiety from the graphene surface.

To begin our experiments, pyrene-appended imidazolium (**PI**) was synthesized, precipitated in KPF_6 (aq.) solution, and washed to provide a white solid as previously reported.[12] Graphene oxide (GO) was prepared by a modified Hummers' method for oxidative exfoliation (details are provided in ESI† along with AFM images in Fig. S1)[13] and was subsequently mixed with SiO_2 particles produced to have an average diameter near 500 nm as described previously. The SiO_2 particles serve an important role as the template for formation of SiO_2@rGO allowing the creation of a high surface area probe for heterogeneous phase detection. Following encapsulation of the silica nanoparticles by simple stirring, the GO was reduced to rGO through addition of hydrazine and the silica particle template was removed by incubation under highly alkaline conditions. The resulting hollow structures were observed by TEM as shown in Fig. 2. In addition, GO wrapped on the surface of SiO_2 particles was confirmed by TEM using an elemental mapping technique (Fig. S2, ESI†). Exposure of 600 pM of **PI** to the high surface area rGO structures allowed capture of **PI** as facilitated by π–π stacking between the pyrene moieties and the rGO surface. A significant amount of **PI** was found to be captured on the surface by the presence of F1s and N1s peaks through XPS (Fig. S3, ESI†). When captured, there is essentially no observable fluorescence from **PI** in the rGO-bound quenched state (Fig. 1C). In contrast, a high fluorescence signal was observed, with the peak residing at ~550 nm, upon exposure to the same concentration of 10-mer (XG_3) DNA. This repeat sequence has the ability to form a G-quadruplex upon complex formation with **PI** resulting in enhanced excimer fluorescence. Interestingly, X_2G_2 and XG_2 dsDNA, which are sequences incapable of G-quadruplex formation, did not elicit any release or complex formation with **PI**, as no significant variation in fluorescence intensity was found for these samples when compared to the quenched off-state of SiO_2@rGO-**PI**.

The dynamic range of our system for detecting G-quadruplex forming dsDNA was investigated using 10-mer (XG_3) dsDNA in 10 mM sodium phosphate buffer (pH = 7.0) (Fig. 3). By observing the fluorescence spectra as a function of target DNA (XG_3) concentration, we found the fluorescence intensity to increase very linearly upon exposure of 20 pM to 140 pM G-quadruplex forming DNA (20 pM being the lowest concentration detected). The maximum signal at 140 pM is attributed to the maximal loading conditions of **PI** onto rGO, as above 140 pM DNA exposure there will be complete complex formation (saturation condition) of target DNA with all available **PI** hence resulting in release and maximal observation of excimer fluorescence. On the basis of these results, our system offers a very significant improvement in terms of sensitivity to G-quadruplex forming DNA.[7,8,20]

In order to gain more information with respect to (XG_3) DNA complex formation with **PI**, we examined different lengths of G-quadruplex forming dsDNA with variation in the number of

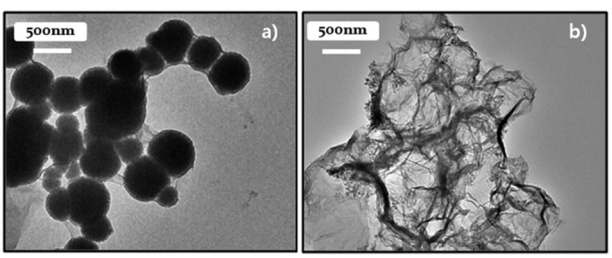

Fig. 2 (a) TEM image of SiO_2@rGO. (b) TEM image of SiO_2@rGO after washing with basic solution (0.1 M NaOH).

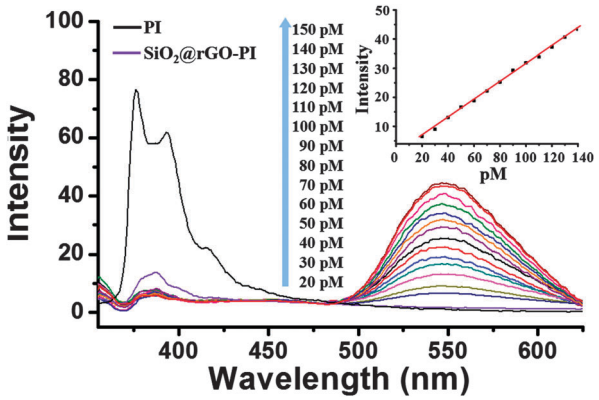

Fig. 3 Fluorescence spectra originating from **PI** and SiO_2@rGO-**PI** upon incubation with XG_3 DNA (0–150 pM). Inset: 550 nm fluorescence intensity as a function of picomolar XG_3 concentration (pM) upon addition to SiO_2@rGO-**PI**.

repeat units. Specifically, we examined 30-mer and 50-mer dsDNA having 6 and 10 repeats of guanosine trimer (G_3) motifs present per DNA duplex (Fig. S4, ESI†), respectively (see ESI† for full DNA sequence details). To provide a frame of reference, the 10-mer (XG_3) DNA mentioned above has only two repeats of (G_3)-motifs present per DNA duplex. Using these dsDNA as a comparison, we found no significant variation in the fluorescence intensity in regard to the number of repeats present per stretch of target DNA. This indicates that an individual DNA molecule will complex with only one molecule of **PI** to form an excimer even if the DNA contains 2–10 repeat units of the (G_3)-motif. Based on prior work examining the specific interactions between **PI** and G-quadruplex forming dsDNA, the interaction of a single molecule of **PI** is expected to require at least two repeating units of the guanosine trimer in the target DNA for effective formation of the G-quartet and induction of excimer fluorescence enhancement,[12] which we also corroborate here (Fig. 1C).

The SiO2@rGO capture platform offers potential for adaptation with other fluorophore based sensing probes. Rhodamine fluorophore conjugates with pyrene, for instance, have already been utilized for selective detection of metal ion species, including Cu^{2+}.[21] Capture of such pyrene conjugates onto SiO_2@rGO may provide similar benefits in high surface area capture as demonstrated in this work. Given the diversity of existing fluorescent signalling probes,[22] integration of such components in the form of pyrene derivatives with our heterogeneous phase capture platform may offer comparable advantages in terms of sensitivity as well as quenching of background fluorescence for enhanced detection. Detection schemes utilizing this type of approach may find higher success in the detection of larger targets, as in our case of G-quadruplex forming DNA, since a sizeable target interaction may be necessary to release the probe from the rGO surface. Because the electronic performance of graphene is sensitive to fluctuations from the surrounding environment,[23] future work on the detection of the controlled release of **PI** by telomeric DNA may make obvious use of a combined electrical/optical readout sensor for enhancing the application diversity.

In conclusion, we have described a vastly improved approach for the detection of G-quadruplex DNA using a fluorescent "turn-on" mode sensor. Extensive capture of **PI** onto high surface area rGO shells provided the means for selective release of **PI** by complex formation with specific DNA sequences resulting in fluorescence enhancement. This unique strategy has succeeded in offering unprecedented sensitivity, in the picomolar range, to G-quadruplex forming DNA, representing a significant advancement in relation to existing techniques. We anticipate that the results of this proof of concept may bring us one step closer to a robust sensor for assessing telomeric DNA in the future by providing a system for quantifying the level of G-quadruplex capable sequence content in a DNA sample. Finally, we expect that the adaptability of this strategy, with respect to new and existing fluorescent probe technologies, may offer the means for implementation of a diverse range of rGO based sensing systems.

This work was supported by a grant from NRF (2012R1A4A1027750 and 2012-002547). In addition, this work was partially supported by a grant from the Next-Generation BioGreen 21 Program (SSAC, grant#: PJ009041022012), Rural Development Administration, Korea.

Notes and references

1 E. H. Blackburn, *FEBS Lett.*, 2005, **579**, 859–862.
2 J. F. Riou, L. Guittat, P. Mailliet, A. Laoui, E. Renou, O. Petitgenet, F. Mégnin-Chanet, C. Hélène and J. L. Mergny, *Proc. Natl. Acad. Sci. U. S. A.*, 2002, **99**, 2672–2677.
3 A. M. Burger, F. Dai, C. M. Schultes, A. P. Reszka, M. J. Moore, J. A. Double and S. Neidle, *Cancer Res.*, 2005, **65**, 1489–1496.
4 H. Tahara, K. Shin-ya, H. Seimiya, H. Yamada, T. Tsuruo and T. Ide, *Oncogene*, 2006, **25**, 1955–1966.
5 P. Phatak, J. C. Cookson, F. Dai, V. Smith, R. B. Gartenhaus, M. F. G. Stevens and A. M. Burger, *Br. J. Cancer*, 2007, **96**, 1223–1233.
6 F. He, Y. Tang, S. Wang, Y. Li and D. Zhu, *J. Am. Chem. Soc.*, 2005, **127**, 12343–12346.
7 C.-C. Chang, I. C. Kuo, I. F. Ling, C.-T. Chen, H.-C. Chen, P.-J. Lou, J.-J. Lin and T.-C. Chang, *Anal. Chem.*, 2004, **76**, 4490–4494.
8 C. Y.-S. Chung and V. W.-W. Yam, *Chem. Sci.*, 2013, **4**, 377–387.
9 R. C. Allsopp, H. Vaziri, C. Patterson, S. Goldstein, E. V. Younglai, A. B. Futcher, C. W. Greider and C. B. Harley, *Proc. Natl. Acad. Sci. U. S. A.*, 1992, **89**, 10114–10118.
10 M. T. Hemann, M. A. Strong, L.-Y. Hao and C. W. Greider, *Cell*, 2001, **107**, 67–78.
11 E. Chang and C. B. Harley, *Proc. Natl. Acad. Sci. U. S. A.*, 1995, **92**, 11190–11194.
12 H. N. Kim, E.-H. Lee, Z. Xu, H.-E. Kim, H.-S. Lee, J.-H. Lee and J. Yoon, *Biomaterials*, 2012, **33**, 2282–2288.
13 J. H. Jung, S.-J. Moon, J. Ahn, J. Jaworski and S. Shinkai, *ACS Nano*, 2013, **7**, 2595–2601.
14 S. Kim, S. H. Ku, S. Y. Lim, J. H. Kim and C. B. Park, *Adv. Mater.*, 2011, **23**, 2009–2014.
15 Y. Chen, F. Guo, Y. Qiu, H. Hu, I. Kulaots, E. Walsh and R. H. Hurt, *ACS Nano*, 2013, **7**, 3744–3753.
16 S. Myung, P. T. Yin, C. Kim, J. Park, A. Solanki, P. I. Reyes, Y. Lu, K. S. Kim and K.-B. Lee, *Adv. Mater.*, 2012, **24**, 6081–6087.
17 S. Myung, A. Solanki, C. Kim, J. Park, K. S. Kim and K.-B. Lee, *Adv. Mater.*, 2011, **23**, 2221–2225.
18 C.-H. Lu, H.-H. Yang, C.-L. Zhu, X. Chen and G.-N. Chen, *Angew. Chem., Int. Ed.*, 2009, **48**, 4785–4787.
19 H. Chang, L. Tang, Y. Wang, J. Jiang and J. Li, *Anal. Chem.*, 2010, **82**, 2341–2346.
20 T. Li, E. Wang and S. Dong, *Anal. Chem.*, 2010, **82**, 7576–7580.
21 Y. Zhou, F. Wang, Y. Kim, S. Kim and J. Yoon, *Org. Lett.*, 2009, **11**, 4442–4445.
22 S. Khatua, S. H. Choi, J. Lee, K. Kim, Y. Do and D. G. Churchill, *Inorg. Chem.*, 2009, **48**, 2993–2999.
23 T. Zhang, Z. Cheng, Y. Wang, Z. Li, C. Wang, Y. Li and Y. Fang, *Nano Lett.*, 2010, **10**, 4738–4741.

